12th IEA Heat Pump Conference 2017

Performance Optimization of Alternative Lower Global Warming Potential Refrigerants in Mini-Split Room Air Conditioners

Bo Shen[a]*, Omar Abdelaziz [a], Som Shrestha [a]

[a]*Oak Ridge National Laboratory, P.O. Box 2008, Oak Ridge, TN 37831, U.S.A.*

Abstract

Oak Ridge National laboratory (ORNL) recently conducted extensive laboratory, drop-in investigations for lower Global Warming Potential (GWP) refrigerants to replace R-22 and R-410A. ORNL studied propane, DR-3, ARM-20B, N-20B and R-444B as lower GWP refrigerant replacement for R-22 in a mini-split room air conditioner (RAC) originally designed for R-22; and, R-32, DR-55, ARM-71A, and L41-2, in a mini-split RAC designed for R-410A. We obtained laboratory testing results with very good energy balance and nominal measurement uncertainty. Drop-in studies are not enough to judge the overall performance of the alternative refrigerants since their thermodynamic and transport properties might favor different heat exchanger configurations, e.g. cross-flow, counter flow, etc. This study compares optimized performances of individual refrigerants using a physics-based system model tools. The DOE/ORNL Heat Pump Design Model (HPDM) was used to model the mini-split RACs by inputting detailed heat exchangers geometries, compressor displacement and efficiencies as well as other relevant system components. The RAC models were calibrated against the lab data for each individual refrigerant. The calibrated models were then used to conduct a design optimization for the cooling performance by varying the compressor displacement to match the required capacity, and changing the number of circuits, refrigerant flow direction, tube diameters, air flow rates in the condenser and evaporator at 100% and 50% cooling capacities. This paper compares the optimized performance results for all alternative refrigerants and highlights best candidates for R-22 and R-410A replacement.

1. Introduction

The use of hydrofluorocarbon (HFC) refrigerants as non-ozone-depleting fluids alternatives for air-conditioning and refrigeration equipment was adopted by the developed countries during the ozone-depleting substances (ODS) phase-out as described in the Montreal Protocol (Ozone Secreteriat, 2016). Unfortunately, the commonly used HFCs have higher global warming potential (GWP) compared to the refrigerants that they replaced, for example, R-410A has a GWP 1924. The transitional hydrochlorofluorocarbons (HCFC) that are still being used in developing countries; such as the popular R-22, has a GWP 1760. Both R-410A and R-22 result in thousands of times higher global warming compared with natural refrigerants like CO_2. HFCs currently account for only 1% of greenhouse gas emissions, but their use is growing rapidly, by as much as 10 to 15% per

Corresponding author. Tel.: +1-865-574-5745; fax: +1-865-574-9338.
E-mail address: shenb@ornl.gov.
© 2017 Stichting HPC 2017. Selection and/or peer-review under responsibility of the organizers of the 12th IEA Heat Pump Conference 2017.

Keywords: Global warming potential, optimization, modelling, room air conditioner

This manuscript has been authored by UT-Battelle, LLC under Contract No. DE-AC05-00OR22725 with the U.S. Department of Energy. The United States Government retains and the publisher, by accepting the article for publication, acknowledges that the United States Government retains a non-exclusive, paid-up, irrevocable, worldwide license to publish or reproduce the published form of this manuscript, or allow others to do so, for United States Government purposes. The Department of Energy will provide public access to these results of federally sponsored research in accordance with the DOE Public Access Plan (http://energy.gov/downloads/doe-public-access-plan).

year, primarily because of their use as replacements for ODS and the increasing use of air conditioners globally, as reported by Ramanathan and Xu (2010 and 2013). Furthermore, according to the Montreal Protocol, Developing Countries, Article 5 Countries, have started their phase-down schedule for ODS. As such, finding suitable lower GWP refrigerants for HFC and HCFC refrigerants is timely and will avoid a costly two-step transition from HCFC to HFC and then from HFC to lower-GWP refrigerants. Therefore, there is potential for significant reduction in greenhouse gas emissions through the substitution of high-GWP HFCs and HCFCs with lower-GWP alternatives.

While progress toward widespread application of lower-GWP refrigerants continues, only limited information regarding the performance of the most commonly proposed lower-GWP refrigerants is available. Abdelaziz and Shrestha (2016) conducted extensive experimental tests to assess low GWP alternative refrigerants as drop-in replacements in two mini-split air conditioning units. One unit was designed for R-22 and the other for R-410A. Table 1 shows the R-22 alternatives; Table 2 shows the R-410A alternatives evaluated in their study. In these tables, the temperature glide in the condenser were calculated as the difference between the saturated vapor temperature and liquid temperature at the pressure corresponding to 115°F (46.1°C) dew point; and glide in the evaporator was calculated at the pressure corresponding to 50°F (18°C) dew point.

Table 1. Alternative Low GWP Replacements for R-22

Refrigerant	GWP AR4	GWP AR5	Safety Class	Glide in Condenser [K]	Glide in Evaporator [K]	Critical Temperature [°C]
R-22	1810	1760	A1	0.0	0.0	96.16
Propane (R-290)	3	3	A3	0.0	0.0	96.74
DR-3[a]	148	146	A2L	6.5	7.7	88.47
ARM-20B[b]	251	251	A2L	5.3	6.0	88.74
N-20B[c]	988	904	A1	4.6	5.4	89.62
R-444B[d]	295	295	A2L	7.6	8.9	92.11

[a] DR-3 has mass-based compositions of R-32 (0.215)/R-1234yf (0.785).
[b] ARM-20B has mass-based compositions of R-32 (0.35)/R-1234yf (0.55)/R-152a (0.1).
[c] N-20B has mass-based compositions of R-32 (0.13)/R-125 (0.13)/R-134a (0.31)/R-1234yf (0.43).
[d] R-444B has mass-based compositions of R-32 (0.415)/ R-1234ze(E) (0.485)/R-152a (0.1).

Table 2. Alternative Low GWP Replacements for R-410A

Refrigerant	GWP AR4	GWP AR5	Safety Class	Glide in Condenser [K]	Glide in Evaporator [K]	Critical Temperature [°C]
R-410A[a]	2088	1924	A1	0.1	0.1	71.34
R-32	675	677	A2L	0.0	0.0	78.12
DR-55[b]	698	676	A2L	1.2	1.3	79.68
ARM-71A[c]	460	461	A2L	1.8	2.1	81.52
L41-2 [d]	583	572	A2L	3.8	4.6	82.63

[a] R-410A has mass-based compositions of R-32 (0.5)/R-125 (0.5).
[b] DR-55 has mass-based compositions of R-32 (0.67)/R-125 (0.07)/R-1234yf (0.26).
[c] ARM-71A has mass-based compositions of R-32 (0.68)/R-1234yf (0.26)/ R-1234ze(E) (0.06).
[d] L41-2, also called R-447A, has mass-based compositions of R-32 (0.68)/R-125 (0.035)/R-1234ze(E) (0.285).

Table 3 compares the R-22 alternatives, while Table 4 compares the R-410A alternatives at the AHRI A condition, i.e. outdoor 35.0°C, indoor 26.7°C dry bulb temperature and 51% relative humidity. Abdelaziz and Shrestha (2016) reported the measured air side capacities and Energy Efficiency Ratios (EER [Btu/h/W]), and compared performances of different refrigerants.

Table 3. Performances of Low GWP Alternatives for R-22

Test Condition	R-22	N-20B	DR-3	ARM-20B	R-444B	Propane

COP	3.07	2.68	2.57	2.71	2.72	3.30
		-13%	-16%	-12%	-11%	+7%
Capacity [kW]	6.10	5.25	5.40	5.91	5.58	5.62
		-14%	-11%	-3%	-9%	-8%

Table 4. Performances of Low GWP Alternatives for R-410A

Test Condition	R-410A	R-32	DR-55	L41-2	ARM-71A
COP	3.40	3.55	3.50	3.22	3.38
		+4%	+3%	-5%	-1%
Capacity [kW]	5.14	5.42	5.01	4.44	4.75
		+5%	-2%	-14%	-8%

As indicated in Table 3, all R-22 alternative refrigerants have smaller cooling capacities, and only propane provides better COP than R-22. Table 4 reveals that R-32 leads to larger capacity and COP than R-410A, and DR-55 leads to similar capacity and COP as R-410A. Other refrigerant drop-ins of the R-410A alternative refrigerants result in smaller capacities and lower COPs at the AHRI A condition.

The drop-in studies are not adequate to compare overall performance of the alternative refrigerants since their thermodynamic and transport properties might favor different heat exchanger configurations, e.g. cross-flow, counter flow, etc. And, a single-speed compressor with a fixed displacement volume leads to difference in capacity up to 10%, and thus, makes the efficiency comparison among the alternative refrigerants invalid, since they don't accomplish the same cooling load. In order to provide a fair comparison, we compare optimized performances of individual refrigerants using a physics-based system model tool. The DOE/ORNL Heat Pump Design Model (HPDM) (Shen and Rice, 2014) was used as the modelling tool to model the mini-split RACs by inputting detailed heat exchangers geometries, compressor displacement and efficiencies as well as other relevant system components. The RAC models were calibrated against the lab data for each refrigerant, as introduced in Shen et al. (2016). The calibrated models were then used to conduct a design optimization for the cooling performance by varying the compressor displacement to match the required capacity, and changing the number of circuits, refrigerant flow direction, tube diameters, air flow rates in the condenser and evaporator at 100% and 50% cooling capacities.

2. Model Description and Calibration

Compressor model: In order to model the alternative refrigerants in one compressor, we used basic efficiencies to model the compressor, i.e. volumetric efficiency shown in Equation 1 to evaluate the refrigerant mass flow rate, and isentropic efficiency shown in Equation 2 to evaluate the compressor power input.

$$\mathrm{m_r} = \mathrm{Volume_{displacement}} \times \mathrm{Speed_{rotation}} \times \mathrm{Density_{suction}} \times \eta_{\mathrm{vol}} \quad \text{(Equation-1)}$$

$$\mathrm{Power} = \mathrm{m_r} \times (\mathrm{H_{discharge,s}} - \mathrm{H_{suction}}) / \eta_{\mathrm{isentropic}} \quad \text{(Equation-2)}$$

Where m_r is compressor mass flow rate; $Power$ is compressor power; η_{vol} is compressor volumetric efficiency; $\eta_{isentropic}$ is compressor isentropic efficiency; $H_{suction}$ is compressor suction enthalpy; $H_{discharge,s}$ is an enthalpy obtained at the compressor discharge pressure and suction entropy.

Heat Exchanger models:

Segment-to-segment fin-&-tube condenser: It uses a segment-to-segment modelling approach, which divides a single tube to numerous mini segments; each tube segment has individual air side and refrigerant side entering states, and considers possible phase transition; An ε-NTU approach is used for heat transfer calculations within each segment. Air-side fin is simplified as an equivalent annular fin. Both refrigerant and air-side heat transfer and pressure drop are considered; the coil model can simulate arbitrary tube and fin geometries and circuitries, any refrigerant side entering and exit states, maldistribution, and accept two-dimensional air side temperature,

humidity and velocity local inputs; the tube circuitry and 2-D boundary conditions are provided by an input file. The flow-pattern-dependent heat transfer correlation published by Thome (2003a, b) is used to calculate the condenser two-phase transfer coefficient. The pressure drop correlation published by Kedzierski (1999) is used to model the two-phase pressure drop.

Segment-to-segment fin-&-tube evaporator: In addition to the functionalities of the segment-to-segment fin-tube condenser, the evaporator model is capable of simulating dehumidification process. The method of Braun et al. (1989) is used to simulate cases of water condensing on an evaporating coil, where the driving potential for heat and mass transfer is the difference between enthalpies of the inlet air and saturated air at the refrigerant temperature. The flow-pattern-dependent heat transfer correlation published by Thome (2002) is used to calculate the evaporator two-phase transfer coefficient. The pressure drop correlation published by Kedzierski (1999) is used to model the two-phase pressure drop. As noted, the segment-to-segment modelling approach is able to reveal the glide of a zeotropic refrigerant, since the temperature increment is accounted by each individual segment along the refrigerant flow path.

Segment-to-segment micro-channel condenser: The model uses a segment-to-segment modelling approach; each micro-channel port segment has individual air-side and refrigerant-side entering states, and considers possible phase transition; the coil model can simulate arbitrary port shapes (round, triangle, etc.), fin geometries and circuitries (serpentine, slab, etc.). The heat transfer correlation published by Dobson (1998) is used to calculate the condenser two-phase heat transfer coefficient. The Kedzierski (2000) correlation is used to calculate the two-phase pressure drop.

Expansion Devices: The compressor suction superheat degree and condenser subcooling degree are explicitly specified. As such, the expansion device is not solved here – a simple assumption of constant enthalpy process is assumed.

Fans and Blowers: Single-speed fan: the air flow rate and power consumption were direct inputs from the laboratory measurements for the model calibration. For the model-based optimizations, fan power consumption is correlated as a function of the air flow rate or frontal velocity.

Refrigerant Lines: Heat transfer in a refrigerant line is ignored and the pressure drop is calculated using a turbulent flow model, as a function of the refrigerant mass flux.

Refrigerant Properties: We programmed interface functions to call REFPROP 9.1 directly; our models accept all the refrigerant types in the REFPROP 9.1 database, and also we can simulate a new refrigerant by making the refrigerant definition file according to the REFPROP 9.1 format, or look-up tables.

Model Calibration:

We modelled the two mini-split RACs, by inputting the exact heat exchanger dimensions and compressor displacement volumes. We calibrated each RAC against the laboratory measurements. HPDM has a flexible solver that any variables can be given or solved. We inputted the measured refrigerant mass flow rate, compressor power, the pressure and temperature measurements at inlets and outlets of individual components, as known variables, and then, solved for the compressor efficiency and the two-phase heat transfer coefficients in the condenser and evaporator as unknowns. Two-step solving procedure was applied to decouple the refrigerant side heat transfer and the air side heat transfer. As the HPDM was validated tremendously against R-22 and R-410A units in previous work (Rice 1997, Shen 2005), and thus, its original refrigerant side heat transfer calculations were considered being accurate for the R-22 and R-410A data. For the first step, we calibrated the air side heat transfer coefficient for the R-22 and R-410A baseline units using the original refrigerant side heat transfer correlations. As the mini-split units have constant indoor and outdoor air flow rates, the air side heat transfer didn't change when running the other alternative refrigerants. For the second step, we treated the calculated air side heat transfer coefficients as knowns, and calculated the refrigerant side two-phase heat transfer coefficients, specific to each alternative refrigerant. The phase allocation ratios, i.e. single-phase versus two-phase, are predicted by the HPDM model. In this case, we have good confidence in correlating air side heat transfer performance specific to the fin and tube type, fin density, etc.; and scaling the fundamentally-based two-phase heat transfer correlations to match the new refrigerants, regardless of coil sizing, flow pattern, fin and tube geometries, etc.

3. Optimization Study

We compared all the refrigerants with modeling study in one RAC, having a rated capacity of 2 tons (7.03 kW), basic information of the condenser and evaporator is described in Table 5.

Table 5: Parameters of a Mini-Split Air Conditioning Unit for Optimization Study

Condenser (outdoor)	Type: Micro-channel

Total Tube Number	65
Number of rows	1
Number of parallel circuits	(47 condensing section + 18 in subcooling)
Fin density [fins/m]	708.7
Frontal flow area [m^2]	0.733
Tube diameter [mm]	0.8 (inside hydraulic diameter)/14 ports
Tube Length [m]	1.185
Evaporator (indoor)	Type: Fin-tube coil
Total Tube Number	30
Number of rows	2
Number of parallel circuits	5
Fin density [fins/m]	787.4
Frontal flow area [m^2]	0.404
Tube outside diameter [mm]	6.3
Tube Length [m]	1.152

We selected best-in-class fans as the outdoor axial fan and the indoor tangential blower. The fan curves are provided below in Figures 1 and 2.

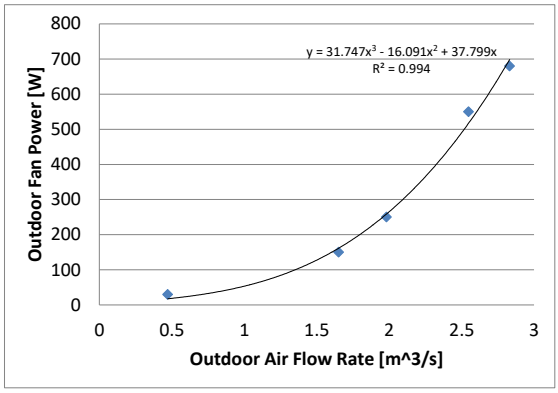


Figure 1. Outdoor axial fan power curve

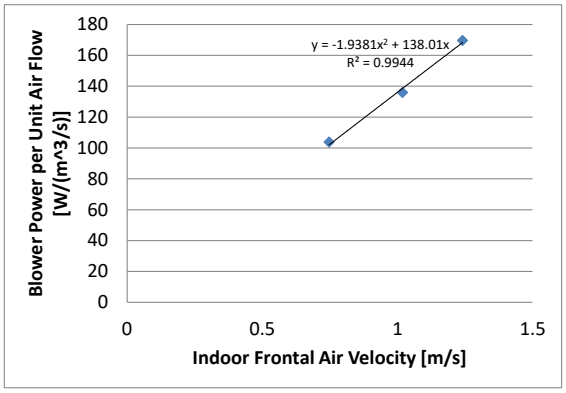


Figure 2. Indoor tangential blower power curve

For the compressor, we assumed a constant compressor isentropic efficiency = 70% and volumetric efficiency = 95% based on our analysis of the previous experimental data; however we allowed the compressor displacement volume to vary in order to match the target capacity for each refrigerant. The compressor suction superheat degree was fixed at 5.6 K. We optimized the unit COP at 35°C ambient air temperature, 26.7°C indoor air temperature and 51% relative humidity, by varying the condenser exit subcooling degree (refrigerant system charge), and indoor and outdoor air flow rates. To provide a fair comparison and locate the optimized configuration of each refrigerant in a large population, we conducted a series of optimization studies as per the following matrix:

- Three evaporator refrigerant flow directions (green cells represent tubes)

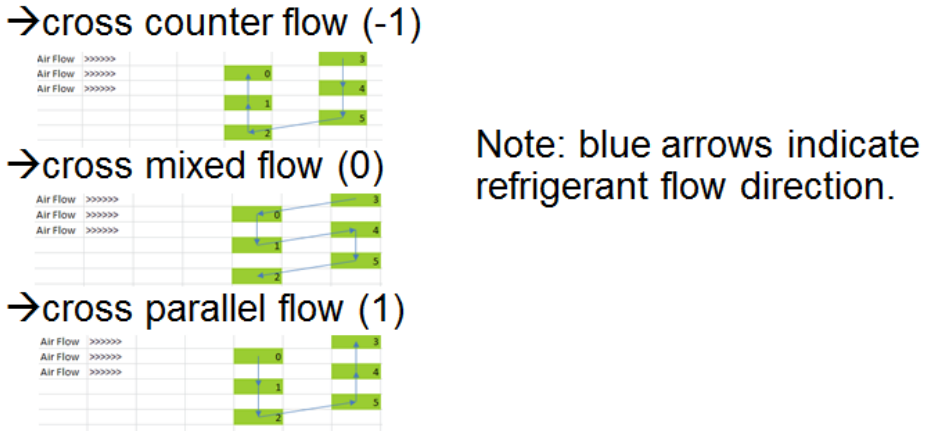


Figure 3. Evaporator flow patterns

- Two evaporator circuit numbers: 5 circuits; 3 circuits (distribute 30 tubes evenly among the circuits)
- Two evaporator tube outside diameters: 6.35 mm; 8.89 mm
- Three tube splits in condenser: 37 tubes (condensing section)/28 tubes (subcooling section); 47/18; 57/8
- Two capacities: 2-ton (7.03 kW, 100% capacity) with sensible heat ratio (SHR) < 75%; 1-ton (3.56 kW, 50% capacity) without SHR limit

Therefore, the population of each refrigerant at one capacity contains 3×2×2×3 = 36 cases. Box-plots are used to show distribution of the optimization cases. Figure 4 illustrates optimized COPs (EERs) of individual refrigerants at 100% and 50% capacities. To be separate from the R-22 alternatives, the R-410A alternative refrigerants are braced. It can be seen that at 100% capacity, half of the R-32 cases are more efficient than the entire R-410A population. DR-55 cases have comparable efficiencies as R-410A. ARM-71a and L41-2 are ranked lower than DR-55. For the R-22 alternatives, if matching the same capacity, R-22 is still the most efficient. The propane's population are actually a bit lower in efficiency. All the other R-22 alternatives have the entire population having lower efficiencies, no matter how the configuration and air flow rates are optimized.

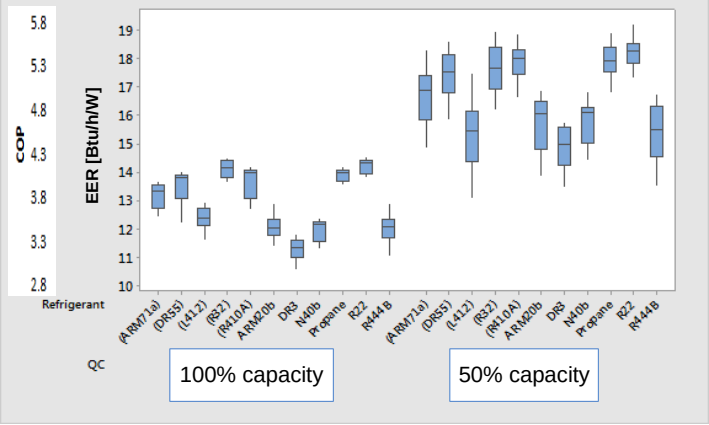


Figure 4. Optimized COPs at 100% and 50% capacities

Figure 5 presents required compressor displacement volumes to match the 100% capacity at the AHRI A test condition. For the R-410A alternatives, R-32 requires smaller displacement volumes, and DR-55 requires similar volumes. As such, R-32 and DR55 are ideal drop-in replacements for R410A, i.e. achieving similar or larger capacities with better COPs in the same compressor. For the R-22 alternatives, ARM-20b requires similar displacement volumes as R-22. However, all the other alternatives have the whole pollution requiring larger compressor displacement volumes. That means that using the same compressor, the ARM-20b drop-in will achieve a similar capacity, but other refrigerants will result in smaller capacities.

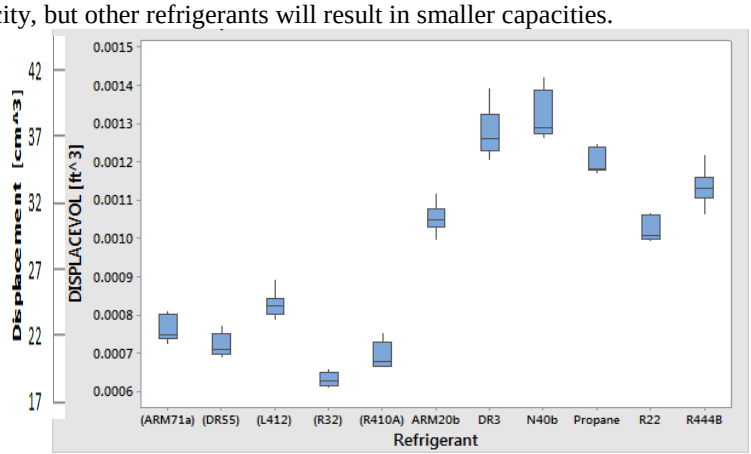


Figure 5. Required compressor displacement volumes at 100% capacity

Figure 6 compares the COPs at the 100% capacity with the three evaporator flow patterns. It is clear that Refrigerants having larger temperature glides prefer cross counter flow arrangement, for example, L41-2 to replace R-410A; and ARM-20b, DR-3, R-444B to replace R-22. On the other hand, the pure refrigerants or mixtures having negligible temperature glides are less sensitive to the evaporator flow patterns since the two-

phase heat transfer is dominated by a nearly constant saturation temperature.

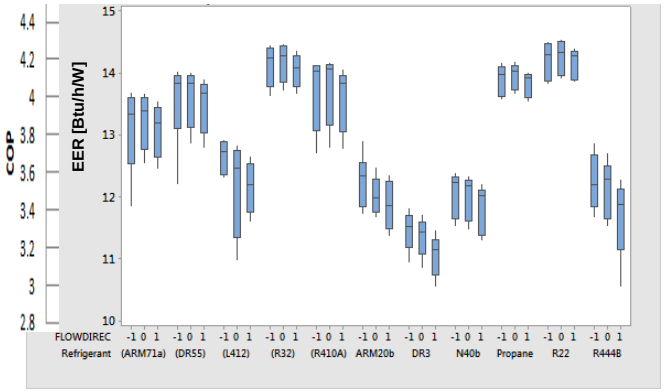


Figure 6. Performances led by different evaporator flow patterns

Figure 7 shows performances led by splitting the evaporator refrigerant flow to three or five circuits. Increasing the circuit number decreases the refrigerant flow velocity, which reduces the evaporator refrigerant pressure drop at the expense of smaller heat transfer coefficient. It indicates, for the R-410A alternatives, the larger number of circuits cause smaller performance dominates other design factors, however, it is opposite for the R-22 alternatives.

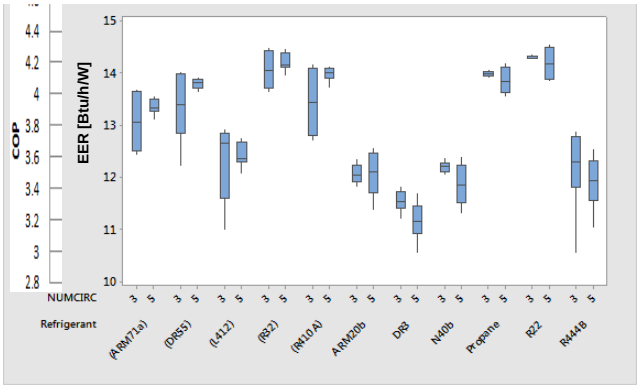


Figure 7. Performances led by different evaporator circuit numbers

Figure 8 illustrates performances led by different evaporator tube diameters. In general, the larger tube results in better performances for all the refrigerants, due to its larger tube surface area. It appears that using a larger diameter tube is more beneficial to the R-22 alternatives than the R410A ones. However, it is important to note that larger tube diameter also impact the refrigerant charge and can have a detrimental impact on the Life Cycle Climate Performance (LCCP) of the unit being designed.

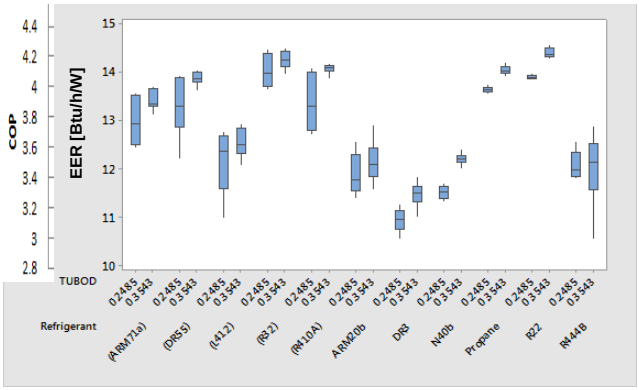


Figure 8. Performances led by different evaporator tube diameters

4. Summary

The cases having maximum COPs with their preferred design options are given in Table 6 for R-22 and its alternative refrigerants and Table 7 for R-410A and its alternative refrigerants. These provide fair comparisons among the lower-GWP refrigerants when matching the same capacity, and using the same number of tubes in the condenser and evaporator. If expecting a similar efficiency level, suitable replacements for R-410A are R-32 and DR-55. On the other hand, propane is the choice for R-22 replacement if the primary focus is on COP (EER). However, being a highly flammable refrigerant limits its field of use. ARM-20b and R-444B provide decent choices for lower GWP alternative refrigerants; especially that they are slightly flammable.

Table 6. Cases having maximum COPs for R-22 alternatives

Refrigerant	R-22	N-20B	DR-3	ARM-20B	R-444B	Propane
Max COP [W/W]	4.26	3.63	3.47	3.78	3.77	4.16
Compressor Disc [cm^3]	28.0	35.7	34.1	28.1	30.0	33.0
Indoor Air Flow [m^3/s]	0.492	0.495	0.491	0.490	0.487	0.491
Outdoor Air Flow [m^3/s]	1.412	1.415	1.415	1.406	1.403	1.415
Subcooling [K]	6.0	5.0	6.6	4.7	4.4	6.8
Evaporator Circuit Number	5	5	3	3	3	5
Evap Tube Diameter [mm]	9.0	9.0	9.0	9.0	9.0	9.0
Evaporator Flow Pattern	Mixed	Counter	Counter	Counter	Counter	Mixed
Condenser Tube Splits	57/8	57/8	47/18	37/28	57/8	57/8

Table 7. Cases having maximum COPs for R-410A alternatives

Refrigerant	R-410A	R-32	DR-55	L41-2	ARM-71A
Max COP [W/W]	4.16	4.24	4.11	3.79	4.01
Compressor Disc [cm^3]	18.7	17.2	19.4	22.2	20.4
Indoor Air Flow [m^3/s]	0.488	0.490	0.487	0.491	0.488
Outdoor Air Flow [m^3/s]	1.415	1.400	1.409	1.381	1.415
Subcoolin [K]	5.9	6.4	6.1	6.6	6.1
Evaporator Circuit Number	3	3	3	3	3
Evap Tube Diameter [mm]	9.0	9.0	9.0	9.0	9.0
Evaporator Flow Pattern	Mixed	Mixed	Counter	Counter	Counter
Condenser Tube Splits	57/8	37/28	37/28	37/28	37/28

Acknowledgements

The authors thank Mr. Antonio Bouza, Technology Development Manager for HVAC, WH, and Appliances, Emerging Technologies Program, Buildings Technology Office; and Ms. Gabrielle Dreyfus, International Climate and Clean Energy Office, at the U.S. Department of Energy for supporting this research project.

References

[1] AHRI. Directory of Certified Product Perfromance. [Online] Air-Conditioning, Heating, and Refrigeration Institute. [Cited: 9 30, 2016.] https://www.ahridirectory.org/.

[2] Abdelaziz, O., and Shrestha S. 2016. Soft-Optimized System Test of Alternative Lower GWP Refrigerants in 1.5-ton Mini-Split Air Conditioning Units. AHRI low-GWP AREP Conference, Jan 2016. http://www.ahrinet.org/App_Content/ahri/files/RESEARCH/AREP_Final_Reports/AHRI_Low_GWP_AREP_Rpt_062.pdf

[3] Braun. J.E., Klein. S.A, and Mitchell, J.W., 1989, "Effectiveness models for cooling towers and cooling coils", ASHRAE Transactions, 95(2), pp. 164-174.

[4] Dobson M. K. and Chato J. C., 1998 "Condensation in Smooth Horizontal Tubes", Journal. Heat Transfer 120(1), 193-213 (Feb 01, 1998)

[5] Kedzierski, M. A., and Choi J. Y., "A generalized pressure drop correlations for evaporation and condensation of alternative refrigerants in smooth and micro-fin tubes" NISTIR 6333, 1999

[6] Lemmon Eric W., Huber Marcia L. (2010) "NIST Reference Fluid Thermodynamic and Transport Properties Database (REFPROP): Version 9.1", http://www.nist.gov/srd/upload/REFPROP9.PDF

[7] Montreal Protocol, An international agreement reached in 1987 to reduce the production and consumption of chlorofluorocarbons (CFCs) and halon substances.

[8] Ozone Secreteriat, 2016, "The 1987 Montreal Protocol on Substances that Depelete the Ozone Layer", UNEP, http://ozone.unep.org/en/handbook-montreal-protocol-substances-deplete-ozone-layer/27571 accessed April 25th 2016.

[9] Ramanathan and Y. Xu (2010). "The Copenhagen Accord for Limiting Global Warming: Criteria, Constraints, and Available Avenues," Proc. Natl. Acad. Sci. USA 107, 8055–8062.

[10] Rice, C.K., 1981, "Design optimization and the limits of steady-state heating efficiency for conventional single speed air-source heat pumps", Contract No. W-7405-eng-26, ORNL/CON-63, Department of Energy; web link: http://web.ornl.gov/~wlj/hpdm/MarkVII.shtml

[11] Shen, B. and Rice, C. K., 2014, HVAC System Optimization with a Component Based System Model – New Version of ORNL Heat Pump Design Model, Purdue HVAC/R Optimization short course, International Compressor & refrigeration conferences at Purdue, Lafayette, USA, 2014; web link: http://hpdmflex.ornl.gov/hpdm/wizard/welcome.php

[12] Shen, B., Shrestha, S and Abdelaziz, O, 2016, "Model Validations for Low-GWP refrigerants in Mini-Split Air Conditioning Units", Science and Technology for the Built Environment, 2016, August, Issue Number: 2374-473

[13] Thome J.R. and Jean Ei Hajal, 2002, "On recent advances in modelling of two-phase flow and heat transfer", 1st Int. Con. on Heat Transfer, Fluid mechanics, and Thermodynamics, Kruger Park, south Africa TJ1, 8-10 April.

[14] Thome J. R., J. El Hajal, and A. Cavallini, 2003a, "Condensation in horizontal tubes, part 1: two-phase flow pattern map", International Journal of Heat and Mass Transfer, 46(18), Pages 3349-3363.

[15] Xu. Y, D. Zaelke, G.J.M. Velders, and V. Ramanathan (2013). "The Role of HFCs in Mitigating 21st Century Climate Change," Atmos. Chem. Phys. 13, 6083–6089.